



Adsorption of successive layers of H₂ molecules on a model copper surface: performances of second to fifth rung exchange-correlation functionals

G. Cilpa, J. Colin, F. Labat, C. Adamo, Gilberte Chambaud

► To cite this version:

G. Cilpa, J. Colin, F. Labat, C. Adamo, Gilberte Chambaud. Adsorption of successive layers of H₂ molecules on a model copper surface: performances of second to fifth rung exchange-correlation functionals. Theoretical Chemistry Accounts: Theory, Computation, and Modeling, 2012, 131 (3), pp.1189. <10.1007/s00214-012-1189-8>. <hal-00789708>

HAL Id: hal-00789708

<https://hal.science/hal-00789708v1>

Submitted on 18 Feb 2013

HAL is a multi-disciplinary open access archive for the deposit and dissemination of scientific research documents, whether they are published or not. The documents may come from teaching and research institutions in France or abroad, or from public or private research centers.

L'archive ouverte pluridisciplinaire **HAL**, est destinée au dépôt et à la diffusion de documents scientifiques de niveau recherche, publiés ou non, émanant des établissements d'enseignement et de recherche français ou étrangers, des laboratoires publics ou privés.



HAL Authorization

**Adsorption of successive layers of H₂ molecules on a model
copper surface: performances of second to fifth rung
exchange-correlation functionals**

Géraldine Cilpa,¹ Jonathan Colin,² Frédéric
Labat,^{2,*} Carlo Adamo,^{2,3} and Gilberte Chambaud¹

¹*Université Paris-Est, Laboratoire Modélisation et Simulation Multi Echelle,
UMR 8208-CNRS, 5 boulevard Descartes, Marne-la-Vallée 77454, France*

²*Laboratoire d'Electrochimie, Chimie des Interfaces et Modélisation pour l'Energie,
UMR CNRS 7575, ENSCP - Chimie Paristech,
11 rue P. et M. Curie, Paris 75231 Cedex 05, France*

³*Institut Universitaire de France, 103 Boulevard Saint Michel, F-75005 Paris, France*

(Dated: January 27, 2012)

Abstract

The interaction of H_2 molecules with a $\text{Cu}(100)$ metallic surface has been investigated by DFT approaches using a $(\text{H}_2)_n\text{Cu}_{13}$ cluster model. Nine exchange-correlation functionals, belonging to the Generalized Gradient Approximations (GGA), meta GGA (mGGA), hybrid Kohn-Sham/Hartree-Fock models, either based on GGAs or mGGAs, range-separated hybrids, and double-hybrid families, have been tested on the chemisorption and physisorption processes involving one or two H_2 layers. The addition of an empirical correction for dispersion has also been tested for some of these functionals. The calculated energies and structural parameters were compared to sophisticated Multi Reference Configuration Interaction including Davidson's correction for quadruple excitations (MRCI+Q).

Our results show that among the nine considered exchange-correlation functionals, none can accurately reproduce all processes involved in the successive layers adsorption. Although an hybrid based on a mGGA such as M06-2X can quantitatively describe both the physisorption step and dissociation barriers involved in the adsorption of the first H_2 , it fails to reproduce its chemisorption. On the other hand, significant discrepancies with the reference post-HF data are obtained for the description of the second layer interaction, no matter which functional is considered, outlining the need of improvement and/or development of exchange-correlation functionals suitable for complex systems such as $\text{H}_2/\text{H}_2\text{Cu}$.

PACS numbers:

Keywords:

I. INTRODUCTION

Molecule-surface interactions have been widely studied, particularly for their interest in catalytic processes. Among them, the H_2 -surface reaction has participated to the understanding of various mechanisms and it is one of the best known activated reaction yielding dissociative chemisorption process. Theoretical approaches have provided deep insights on the chemical phenomenon¹. Many studies have focused on the adsorption of H_2 on clean copper surfaces and most of them were concerned with the dissociative chemisorption and the subtle effects governing the dissociation on surfaces. Using multi-dimensional Potential Energy Surfaces (2D, 4D and 6D PES) to describe the interaction potential, the dynamics of the chemisorption have been studied, taking into account the effects of the molecular ro-vibrational excitations on the dissociation, the scattering, the sticking probabilities, the anisotropy of the energy, the corrugative effects and the reactivity at surfaces²⁻⁹.

In most of these studies, the surface is described by a periodic 2D-representation, namely a slab representation, calculations being performed using Density Functional Theory (DFT) methods with H_2 molecules either bound to the surface or very close to it (distances are smaller than 4 bohr). Alternative studies have also been performed, modeling the surface by a cluster. In such cases, the size of the cluster plays a relevant role since it influences the reactivity of the metal towards H_2 , as demonstrated by Raghavan *et al.*¹⁰ in the case of D_2/Ni , and also the quality of the results¹¹. Moreover, it has been shown that, in the case of Cu, 3D metallic clusters⁷ with more than 6 atoms can satisfactorily reproduce the experimental interatomic distances¹². Similar conclusions were obtained by Siegbahn *et al.*¹³ for Ni clusters with even (14) and odd (13) numbers of metallic atoms and one H_2 molecule. On the other hand, the convergence of the adsorption energy with the cluster size¹⁴ is more problematic. Despite the large amount of theoretical works, some questions still remain, especially concerning the energetics of H_2 molecules interacting with a metallic surface already covered with a first layer of hydrogens. In a recent theoretical study on the H_2/Cu system¹⁵ using a cluster model consisting of 13 Cu atoms, it has been shown that the chemisorption and physisorption of the first H_2 layer and the van der Waals (vdW) interactions responsible for the physisorption of additional H_2 layers can be satisfactorily reproduced by highly correlated electronic wavefunctions. Unfortunately, such refined approaches cannot be easily used in large or extended (2D, 3D) systems and other possibilities must be explored.

Density functional theory techniques have been shown to be robust and reliable for the accurate evaluation of a large number of chemical and physical properties in different phases ranging from single molecules to solid states^{16,17}. Therefore, it appeared interesting to investigate the behaviour of different DFT models for such an intriguing system, $(\text{H}_2)_n\text{Cu}_{13}$. Several DFT studies have already been devoted to the specific problem of the interaction of one H_2 molecule with metallic surfaces, but more questionable is indeed the DFT description of the interaction of a second layer of H_2 molecules with the surface. This weak interaction is ruled by vdW forces and it is well known that standard exchange-correlation functionals provide a poor description of such dispersion interactions. Recent studies have shown, however, that sophisticated DFT approaches can give promising outcomes for such difficult cases. In this sense, meta-GGA models (see below) give interesting results for quantitative reproduction of weak interactions in small model systems like rare-gas dimers^{18,19} or in biological molecules²⁰. More recently, the introduction of a perturbative second-order contribution in the DFT framework, through a semiempirical mixing, seems to be another promising route for vdW systems, even if, as for its predecessors it has been tested only on model systems²¹. More easily, addition of an empirical correction to a reparametrized functional²¹ is another possibility, which has already been successfully applied to numerous weakly-interacting systems^{22–24}.

The goal of the present work is thus to extend this study on weak interactions by considering a more complex (and chemically interesting) system, $(\text{H}_2)_n\text{Cu}_{13}$, in which interactions of different nature (physisorption and chemisorption) occur and to assess the performances of different exchange-correlation functionals for the description of such a system.

II. EXCHANGE-CORRELATION FUNCTIONALS

In this section, we give a brief survey of the different classes of functionals selected for the present study. They belong to the second, third, fourth and fifth levels of the so-called five level Jacob’s ladder²⁵, which goes from local to fully non-local functionals, suggesting a complexity and quality improvement when climbing the different levels. Extensive literature is available on this subject (see Ref. 26 for instance).

In the second level, Generalized Gradient Approximation (GGA) functionals include dependence on the electronic density ρ and its gradient $\nabla\rho$. Density functional theory with

GGA includes self-exchange and self-correlation, both being unphysical²⁶. Self-correlation can be eliminated in the next level, by including an additional dependence on the Laplacian of the density $\Delta\rho$ or on the kinetic energy density in meta-GGAs. Self-exchange on the other hand can be removed by adding a fraction of non-local Hartree-Fock (HF) exchange in the expression of the energy of a GGA or a mGGA, constituting the so-called hybrid functionals in the fourth level. Finally, in the fifth level, double hybrid functionals such as B2PLYP²⁷ replace a fraction of the semi-local correlation energy by a non-local correlation energy expression that employs the Kohn-Sham orbitals in second-order many-body perturbation theory.

Global GGA hybrids (GH, such as B3LYP²⁸ or PBE0^{29,30}), which include a *constant* percentage of HF exchange that is mixed with density functional exchange, are probably the most popular functionals since they tend to improve GGA or mGGA computed properties, both for molecular and solid-state systems. In some cases however, *range-separated hybrids* (RSH), in which the Coulomb operator is usually separated in a short- and a long-range part with varying amounts of HF exchange depending on the point in space, perform better.

In this paper, nine functionals have been considered: (i) PW91PW91³¹ (referred to as PW91 in the following), a GGA which is well-known to significantly overestimate van der Waals interactions^{32,33}; (ii) a dispersion-corrected GGA (B97-D³⁴), based on a reparametrized B97 functional³⁵ and including damped atom-pairwise dispersion corrections, commonly used as a reference in the modeling of weakly-interacting systems; (iii) two popular hybrid GGAs, B3LYP²⁸ and PBE0^{29,30}, the first typically predicting unbound systems for this kind of interactions³⁶ while the latter has already been shown to give better results^{18,21}; (iv) M06-L³⁷, a mGGA parametrized on a diverse set of data including non-covalent interactions; (v) an hybrid mGGA, M06-2X³⁸, aimed at an accurate description of both thermochemistry and nonbonded interactions with 54% of HF exchange; (vi) two RSH, ω B97X³⁹ and ω B97XD⁴⁰, including 15.77% and 100% of HF exchange at short- and long-range, respectively, with an additional empirical dispersion correction for the latter, which has already been successfully applied to the treatment of non-covalent interactions⁴⁰; (vii) B2PLYP²⁷, a double hybrid belonging to the fifth level of the Jacob’s ladder, which has already been shown to poorly describe the π stacking of the benzene dimer for instance²¹.

For the sake of clarity, we note that the empirical dispersion contribution in the B-97D and ω B97XD functionals differ in two ways: a scaled contribution is used in the former, while it

is not in the latter, and different dispersion parameters are also considered.

III. COMPUTATIONAL DETAILS

The metallic surface corresponding to a (100) crystal face is described by a cluster containing 13 atoms of Cu : 9 on the first layer interacting with the H₂ molecule, and 4 below. A rigid unrelaxed cluster model, in which distances between Cu atoms are kept fixed at their solid state values, has been chosen, since relaxation of such a system could induce spurious effects. This model is similar to the one used in a recent theoretical study¹⁵ whose results are compared to the present ones.

All calculations have been carried out with the latest available commercial version of the Gaussian code⁴¹, using an effective core potential (ECP) and associated basis set developed by the Stuttgart group⁴² for Cu (19 electrons are treated explicitly, (3s² 3p⁶ 3d¹⁰ 4s¹)), while a large diffuse basis set 6-311++G(3df,3pd)⁴³⁻⁴⁶ is chosen for the hydrogen atoms in order to insure a proper description of the negative H^{δ-} on the metallic surface.

For symmetry reasons, the position of the center of mass of H₂ has been constrained along the z axis, perpendicular to the surface at the center of the central Cu atom. The dissociation path investigated for the first H₂ molecule proceeds along the bridge-top-bridge(*btb*) orientation, as described in Figure 1, where the center of mass of H₂ is on a top site and H atoms are dissociating on bridge sites. According to recent calculations by Kokh *et al.*⁴⁷ employing the embedded cluster model and highly correlated wavefunctions, even though hollow sites are energetically favored for most of the molecular chemisorbed species, the difference in the binding energies between hollow, top and bridge sites is rather small if the bond has a large fraction of ionic character, which is the case in the present situation. Such results confirmed the DFT calculations of Eichler *et al.*⁴⁸ who found an energy difference smaller than 0.1 eV between the binding energies in hollow or bridge sites. Since the different sites of chemisorption have roughly the same energy and correspond to stable or metastable minima, we have chosen to work here with the *btb* orientation of the H₂ molecule because it allows additional symmetry simplifications within our cluster model. Two degrees of freedom have been investigated, *Z* the distance of the center of mass of H₂ to the center of the central Cu atom, and *d* the intramolecular H-H bond distance. In the present work, we neglect the rotations of the first H₂ molecule, in particular we have fixed the molecular

axis parallel to the surface, which is the most favorable orientation for the dissociation of the H_2 molecule. For the second layer of H_2 molecules, two orientations are selected: one with the molecular axis of H_2 parallel to the surface and to the first molecule, and the other one with the molecular axis perpendicular to the surface. These systems are depicted in Figure 2, respectively. For each value of the distance Z , the H_2 bond length d has been optimized. On this 2D-Potential Energy Surface, the corresponding stationary points give the minimum energy pathway of H_2 along the z axis perpendicular to the cluster surface. The reference zero energy is defined as the sum of the energy of the free H_2 molecule and the energy of the bare Cu_{13} cluster.

In the DFT calculations, the contamination of the electronic state has been monitored through the expectation value of the S^2 operator, $\langle S^2 \rangle$, whose value was always close to 0.75 for all the physisorption processes (with one or two H_2 molecules). More involved is the situation for the chemisorption since two electronic states, namely $^2\text{A}_1$ and $^2\text{B}_2$ are very close in energy. For instance, their energy difference at the equilibrium geometry is about 0.1 eV at the B3LYP level. This is in line with a previous work carried out by some of us on $(\text{H}_2)_n/\text{Ag}_{13}$ ⁴⁹, in which it was shown that several electronic states were interacting in the vicinity of the activation barrier, leading to complex electronic structures. Following the previous MRCI study, only the $^2\text{A}_1$ state has been considered in this work. Moreover, we want to notice that it was not possible to compute energies with the same basis used for the MRCI calculations due to problems related to the errors of the numerical integration for the exchange-correlation contribution to the total energy. In addition, the Basis Set Superposition Error (BSSE) has not been evaluated in order to make our DFT calculations directly comparable to the MRCI calculations, carried out under similar conditions¹⁵. In the MRCI+Q calculations, it is rather small in the present H_2/Cu system and estimated to 4.10^{-4} eV close to the minimum of physisorption, namely smaller than the expected accuracy of the MRCI calculation, which is rather in the range of 10^{-3} eV. With all considered DFT methods on the other hand, it is found below 0.1 eV.

IV. RESULTS AND DISCUSSION

A. First layer interaction

In the study of the interaction of H_2 with the copper surface, three different steps are easily identified, namely, the physisorption, the formation of the transition state and the chemisorption. These steps are analyzed and discussed separately because they involve electronic effects of different nature. Interaction energies (E), dihydrogen bond lengths ($d(H-H)$) and distance from the cluster surface (Z) are displayed in Table-I and compared to available data^{7,15}.

1. Physisorption

An experimental physisorption energy of approximately 30 meV has been deduced from scattering experiments and selective adsorption measurements by Andersson *et al.*^{50,51}. From the data given in Table-I one can see that the MRCI calculations¹⁵ including the Davidson correction (MRCI+Q) are in excellent agreement with experimental results, they concluded to the existence of a shallow physisorption minimum located far from the surface, at about 7.0 bohr. Typical shape of the potential energy curve of interacting fragments is obtained in Fig. 3 for all methods: repulsive component at short-range, followed by an attractive component at larger distances, with more or less deep wells.

We can first note that since the physisorption interaction does not change dramatically the internal structure of the H_2 molecule, it is not surprising that the $d(H-H)$ data are weakly sensitive to the choice of the theoretical model, all methods providing very close results. On the other hand, vertical distances (Z) and interaction energies are much more functional-dependent. In particular, computed interaction energies range between 1.1 and 38 meV, the $\omega B97X$, $\omega B97XD$ and M06-2X functionals giving an error below 3 meV with respect to the MRCI+Q data, outperforming the original B97-D functional often used as a reference in the modeling of weakly-interacting systems. The largest errors are obtained at the GH level for the interaction energies, B3LYP predicting almost unbound H_2 and PBE0 slightly improving the description. Interestingly, we note that a standard GGA functional such as PW91 underestimates the MRCI+Q value of about the same amount as the B97-D functional overestimates it.

The MRCI+Q vertical distance (Z) is only quantitatively reproduced at the M06-2X level, a GmH parametrized on a diverse set of data including non-covalent interactions, all other functionals predicting either too small (B97-D, ω B97X, ω B97XD, M06-L) or too large (PW91, PBE0, B3LYP) values. This is especially true for these two latter functionals for which computed errors with respect to the MRCI+Q data are larger than 1 bohr.

Surprisingly, we note that a mGGA such as M06-L poorly describes such an interaction, with significant errors of about 10 meV on the interaction energy and 0.6 bohr on the Z parameter. This might be related to the sawtooth shape of the M06-L curve around the minimum in Fig. 3, due to the default integration grid used. Finally, we note that significant differences are obtained in the shape of the energy profiles in the region between 10 and 12 bohr. In particular, the only functional reproducing nicely the MRCI+Q profile is ω B97X, all other functionals leading to too steep or too flat curves. At larger distances ($Z > 12$ bohr), the interaction is also poorly described with an underestimation of the interaction with all functionals.

The B2PLYP approach deserves a separate comment since it leads to unphysical results, characterized by large (> 1 Hartree) interaction energies. A deep analysis of the numerical data suggests that correct energies are obtained for the hybrid part of the functional, which is close to those provided by similar functionals, like B3LYP, while the erroneous values arise from the perturbative correlation corrections. This error could confirm that, at least in our case, the Kohn-Sham Hamiltonian is not the optimal choice for the perturbation expansion⁵². The same behaviour has been found for the other systems studied in the present paper so that the results obtained with the B2PLYP functionals are not discussed or reported in the tables.

To sum up, physisorption of the first H_2 molecule on the Cu_{13} cluster represents a challenging system for DFT. Although a nice agreement with the MRCI+Q data can be obtained with some functionals, only one (M06-2X) simultaneously quantitatively reproduces the three chosen parameters (interaction energy, vertical H_2/Cu_{13} distance and H-H distance) characterizing this process. At large cluster/ H_2 distances however, it fails to reproduce the MRCI+Q curve, predicting too steep curve in the 10-12 bohr region, and underestimating the interaction energy above.

2. Transition barrier

When the H_2 molecule approaches the surface and is close enough to experience the attractive potential of the substrate, its bond weakens and the two atoms are pulled apart before being chemisorbed, due to an electron donation of the Cu_{13} cluster in the first anti-bonding orbital of H_2 . As previously-shown in several studies on $\text{H}_2/\text{Cu}(100)^{7,8}$, the molecule has to get over a barrier for the dissociation. This barrier is very sensitive to the models, and depends on: (i) the surface coverage, (ii) the number of integration points in the \mathbf{k} -space for periodic calculations, (iii) the atomic basis set, (iv) the method used to represent the core electrons (pseudopotential or frozen core). Investigations on both systems ($\text{H}_2/\text{Cu}(100)$ and $\text{H}_2/\text{Cu}(111)$) already suggested that GGA methods with a periodic slab approach overestimate barriers for $\text{H}_2 + \text{Cu}$ systems by about 0.1-0.2 eV⁵³. These latter results mean that, according to Wiesenekker estimates (0.7 eV)⁷, the barrier height would be rather about 0.5-0.6 eV and the difference between GGA/slab and MRCI+Q calculations would thus be large. Dynamical calculations carried out by Somers *et al.*⁴ using a potential-energy surface fitted on periodic GGA results are in line with the work of Wiesenekker *et al.*⁷ (see Table-I).

In the present work, the same cluster as already considered in the previous MRCI calculations¹⁵ has been used to model the copper surface, making a comparison with these reference post-HF data easier than with the DFT periodic works. The energy range covered by the chosen functionals is [0.81, 1.56] eV, all functionals underestimating the barrier height if we except the M06-2X data. The lowest barriers and largest errors are computed at the M06-L and PW91 levels, the value obtained with this latter functional being in line with previously-published periodic calculations⁸. All functionals including exact HF exchange improve the agreement with the reference post-HF data, an almost perfect agreement being obtained at the M06-2X level.

The positions of the barrier along the z axis are all slightly overestimated with a difference of about 0.28 bohr on Z (for the highest with M06-L) and about 0.16 bohr (for the lowest with M06-2X) with respect to the MRCI+Q calculations, all functionals performing nicely for the determination of the dissociation barrier.

Summarizing, we can say that DFT and MRCI+Q calculations are comparable for this process, with an overall better agreement when using a GmH functional such as M06-2X.

3. Chemisorption

For the dissociative chemisorption of H_2 on Cu, all functionals give similar equilibrium distances Z , slightly below 2 bohr. This distance is in excellent agreement with that obtained at the MRCI level or using periodic calculations within a GGA approach⁷ (1.9 and 2.0 bohr, respectively). The agreement on the optimized H-H bond length is also quite satisfactory, the d value ranging between 4.57 (ωB97X) and 4.85 bohr (M06-L), with a reference post-HF value of 4.82 bohr.

The difference in the chemisorption energy between the MRCI and periodic approaches is typically of about 0.1-0.2 eV, which can be assigned to different reasons. In particular, in periodic calculations, due to interatomic interaction between H_2 molecules in the adlayer⁷, the mean energy of one H_2 interacting with the unit cell of the surface is not equal to the energy of a single H_2 with the surface⁶. The results of Guvelioglu *et al.*⁵⁴ for the chemisorption energy of H_2 interacting with the Cu(100) surface confirm Wiesenekker *et al.*⁷ energy value which is found to be around 0.5 eV. Overestimated energies when dealing with clusters have also been reported by Guvelioglu *et al.*⁵⁴ who have calculated dissociative chemisorption energy of H_2 for optimized Cu_n of different sizes, n varying from 2 to 15. The chemisorption interaction for clusters of n greater than 12 converges slowly to values within the range 0.6-0.9 eV.

Computed chemisorption energies are very similar with all methods, except for the M06-2X functional which significantly underestimates the MRCI+Q value. From Table-I, it is clear that all computed values are lower than the post-HF reference data, if we except the PW91 value for which an excellent agreement with previous periodic works is nevertheless obtained. All functionals perform very well, except M06-2X for which a significant underestimation of the chemisorption energy is obtained. Since functionals including 20 to 25% of HF exchange already reproduce nicely the MRCI+Q value, we can probably relate this discrepancy to the larger percentage included in M06-2X (54%) compared to other hybrids. On the other hand, the comparison with the two considered RSH (ωB97X and ωB97XD) is not straightforward, since their amount of HF exchange is not constant. A quantitative agreement with the MRCI+Q value is obtained at the M06-L and B97-D levels, that is with functionals which only include approximated exchange. In addition, the post-HF vertical distance (Z) is well-reproduced by all DFT methods, if we except once again the M06-2X

functional.

In summary, among the nine functionals considered, none could be found to quantitatively reproduce the MRCI+Q data for the adsorption of one H_2 molecule on a model copper surface. Although M06-2X nicely performs both for the physisorption and energy barrier data, it surprisingly fails to reproduce the chemisorption. This might be related to its large amount of exact HF exchange, which is well-known to provide large errors on geometrical parameters, thus affecting, as in the present case, the energetical features.

B. Second layer interaction

The second layer interaction is described as the interaction of an incoming H_2 with the chemisorbed system at its equilibrium geometry $\text{H}+\text{H}+\text{Cu}_{13}$ ($Z=1.9$ bohr and d about 4.80 bohr depending on the considered functional). Two approaches of the second H_2 molecule have been investigated: *parallel* or *perpendicular* to the first adsorbed H_2 , see Figures 2 and 2, respectively.

The previous MRCI+Q calculations¹⁵ are the only existing reference calculations for this process : they have shown that the incoming hydrogen molecule in this second layer is not dissociated and only slightly activated, with a negligible stretching of the H-H bond. Table II presents data computed for both approaches of the second H_2 molecule.

1. Parallel approach

The results for the physisorption along this orientation can be directly compared to those of the first layer since the H_2 molecule approaches the surface in the same way. The comparison of the two sets of data given in Tables I and II shows that, for all functionals, the physisorption interaction of the second layer is smaller than that of the first layer, giving longer Z distances and smaller interaction energies. This is not in agreement with the MRCI+Q data, for which the opposite behavior is obtained.

From Fig. 4, it is clear that all functionals considered fail to accurately reproduce the post-HF curve. In particular, computed DFT interaction energies range between 0.3 (B3LYP) and 19.8 meV (B97-D), corresponding to vertical distances Z of 10.11 and 7.99 bohr, that is significantly different from the 77.5 meV and 6.42 bohr values computed at the MRCI+Q

level. In fact, all functionals underbind the second H_2 molecule of at least 60 meV and predict too large Z parameters of at least 1.5 bohr. This is especially true for B3LYP, for which the conclusions drawn for the adsorption of the first H_2 layer still hold, with a very shallow profile in this case. It is interesting to notice that very similar interaction energies are computed at the ωB97X and ωB97XD levels, outlining that, around the physisorption minimum obtained with these functionals, dispersion only plays a small role, the two profiles being notably different only at larger Z distances.

On the other hand, the H_2 d bond length at the minimum of the physisorption well shows that H_2 is not dissociated but only slightly stretched, in agreement with the MRCI+Q results.

2. *Perpendicular approach*

In complete agreement with previous MRCI+Q results, for all functionals, calculated interaction energies upon perpendicular approach are larger than those obtained when considering a parallel approach, except for B97-D for which a reverse trend is surprisingly obtained.

As noticed for the parallel approach, significant discrepancies are obtained at the DFT and MRCI+Q levels, with smaller interaction energies and larger equilibrium distances Z computed with the former techniques. These trends clearly appear in Fig. 4.

C. Comments

The analysis of the above discussed results is not straightforward since no trends are clearly evident in going from first to second layer interactions and from chemi- to physisorption. Nevertheless, some points can be underlined.

Although the physisorption and dissociation processes involved in the adsorption of the first H_2 molecule on the copper surface can be accurately described by a GmH functional such as M06-2X, this functional fails to reproduce the MRCI+Q data for the chemisorption. A more balanced description on such problems can be obtained with *ab initio* multiconfigurational methods, but these techniques are rapidly limited by the number of atoms and electrons to be considered. Description of the physisorption of the second H_2 layer is however much more challenging. In contrast to the MRCI+Q results, computed DFT interaction

energies for this layer are smaller than those calculated for the first one. This stems probably from the fact that the DFT cannot reproduce the polarization of the surface due to the first chemisorbed layer as shown by the very small dipole moment calculated at the equilibrium geometry of the $\text{H}+\text{H}+\text{Cu}_{13}$ chemisorbed system. Consequently, there is no enhancement of the second layer interaction. This suggests that the second layer H_2 molecule does not experience any significant distortion of its electronic cloud from the underlying system $\text{H}+\text{H}+\text{Cu}_{13}$.

From a more general viewpoint, it should also be noticed that functionals providing accurate results on small model systems show their limits when applied to larger and more complex systems, such as the one considered in the present study.

D. Conclusions

In this paper, the interaction of H_2 with a metallic Cu cluster has been studied at DFT level. Nine exchange-correlation functionals, belonging to the Generalized Gradient Approximations (GGA), meta GGA (mGGA), hybrid Kohn-Sham/Hartree-Fock models, either based on GGAs or mGGAs, range-separated hybrids (RSH), and double-hybrid families, have been tested on the chemisorption and physisorption processes involving one or two H_2 layers. The addition of an empirical correction for dispersion has also been tested for some of these functionals. Comparison has been made with previously-reported accurate Multi Reference Configuration Interaction data.

Although the physisorption and dissociation processes involved in the adsorption of the first H_2 molecule can be accurately described by a GmH functional such as M06-2X, this functional fails to reproduce the post-HF data for the chemisorption step. Thus, among the nine tested DFT methods, none reproduced quantitatively the MRCI+Q values.

More critical is the description of the second H_2 layer, for which significant discrepancies on both physisorption energies and positions have been found with all DFT methods, no matter if a parallel or a perpendicular approach of the second H_2 molecule with respect to the first one is considered. In particular, all these methods predict interaction energies smaller than the computed physisorption energies of the first layer, in contrast to the post-HF data for which a reverse trend is obtained. This has been attributed to a poor description of the polarization of the surface due to the first chemisorbed layer, as outlined by the very

small dipole moments calculated at the equilibrium geometry of the $\text{H}+\text{H}+\text{Cu}_{13}$ chemisorbed system.

From these results therefore, although recently-developed DFT methods can be successfully applied to small or medium-sized weakly-interacting systems, their application to larger or more complex systems such as $\text{H}_2/\text{H}_2\text{Cu}_{13}$ is still challenging, opening the route for improvement and/or development of exchange-correlation functionals suitable for such systems.

* Electronic address: frederic-labat@chimie-paristech.fr

- ¹ A. Groß, Surf. Sci. **32**, 291 (1998).
- ² G. R. Darling, J. Chem. Phys. **101**, 3268 (1994).
- ³ E. Watts and G. O. Sitz, J. Chem. Phys. **114**, 4171 (2001).
- ⁴ M. F. Somers, R. A. Olsen, H. F. Busnengo and G. J. Kroes, J. Chem. Phys. **121**, 11379 (2004).
- ⁵ W. A. Diño, H. Kaisai and A. Okiji, Prog. Surf. Sci. **63**, 63 (2000).
- ⁶ G. Wiesenekker, G. J. Kroes, E. J. Baerends and R. C. Mowrey, J. Chem. Phys. **102**, 3873 (1995).
- ⁷ G. Wiesenekker, G. J. Kroes and E. J. Baerends, J. Chem. Phys. **104**, 7344 (1996).
- ⁸ J. A. White and D. M. Bird, Phys. Rev. Lett. **73**, 1404 (1994).
- ⁹ P. Kratzer, B. Hammer and J. K. Nørskov, Surf. Sci. **359**, 45 (1996).
- ¹⁰ K. Raghavan, M. S. Stave and A. E. DePristo, J. Chem. Phys. **91**, 1904 (1999).
- ¹¹ D. Dominguez-Ariza, C. Sousa, N. M. Harrison, M. V. Ganduglia-Pirovano and F. Illas, Surf. Sci. **522**, 185 (2003).
- ¹² P. Jaque and A. Toro-Labbé, J. Chem. Phys. **117**, 3208 (2002).
- ¹³ P. E.M. Siegbahn, M. R.A. Blomberg and C. W. Bauschlicher Jr., J. Chem. Phys. **81**, 2103 (1984).
- ¹⁴ J. L. Whitten and H. Yang, Surf. Sci. Rep. **24**, 55 (1996).
- ¹⁵ G. Cilpa and G. Chambaud, Surf. Sci. **601**, 320 (2007).
- ¹⁶ R. O. Jones and O. Gunnarsson, Rev. Mod. Phys. **61**, 689 (1989).
- ¹⁷ S. Kurth, J. P. Perdew and P. Blaha, Int. J. Quant. Chem. **75**, 889 (1999).
- ¹⁸ J. Tao and J. P. Perdew, J. Chem. Phys. **122**, 114102 (2005).

- ¹⁹ C. Adamo and V. Barone, J. Chem. Phys. **108**, 664 (1998).
- ²⁰ Y. Zhao and D. G. Truhlar, J. Chem. Theor. Comput. **3**, 289 (2007).
- ²¹ S. Grimme, J. Chem. Phys. **124**, 34108 (2006).
- ²² S. Grimme, J. Comput. Chem. **25**, 1463 (2004).
- ²³ R. Huenerbein, B. Schirmer, J. Moellmann and S. Grimme, Phys. Chem. Chem. Phys. **12**, 6940 (2010).
- ²⁴ A. Krishtal, K. Vanommeslaeghe, A. Olsaz, T. Veszprémi, C. Van Alsenoy and P. Geerlings, J. Chem. Phys. **130**, 174101 (2009).
- ²⁵ J. P. Perdew and A. Ruzsinszky and J. Tao and V. N. Staroverov and G. E. Scuseria and G. I. Csonka, J. Chem. Phys. **123**, 62201 (2005).
- ²⁶ C. J. Cramer and D. G. Truhlar, Phys. Chem. Chem. Phys. **11**, 10757 (2009).
- ²⁷ S. Grimme, J. Chem. Phys. **124**, 34108 (2006).
- ²⁸ P. J. Stephens and F. J. Devlin and C. F. Chabalowski and M. J. Frisch, J. Phys, Chem. **98**, 11623 (1994).
- ²⁹ C. Adamo and V. Barone, J. Chem. Phys. **110**, 6158 (1999).
- ³⁰ M. Ernzerhof and G.E. Scuseria, J. Chem. Phys. **110**, 5029 (1999).
- ³¹ J. P. Perdew and J. A. Chevary and S. H. Vosko and K. A. Jackson and M. R. Pederson and D. J. Singh and C. Fiolhais, Phys. Rev. B **46**, 6671 (1992).
- ³² D. C. Patton and M. R. Pederson, Phys. Rev. A **56**, 2495 (1997).
- ³³ E. R. Johnson and G. A. Dilabio, Chem. Phys. Lett. **419**, 333 (2006).
- ³⁴ S. Grimme, J. Comput. Chem. **27**, 1787 (2006).
- ³⁵ A. D. Becke, J. Chem. Phys. **107**, 8554 (1997).
- ³⁶ S. Tsuzuki and H.P. Lüthi, J. Chem. Phys. **114**, 3949–3957 (2001).
- ³⁷ Y. Zhao and D. G. Truhlar, J. Chem. Phys. **125**, 194101 (2006).
- ³⁸ Y. Zhao and D. G. Truhlar, Theor. Chem. Acta **120**, 215 (2008).
- ³⁹ J.-D. Chai and M. Head-Gordon, J. Chem. Phys. **128**, 084106 (2008).
- ⁴⁰ J.-D. Chai and M. Head-Gordon, Phys. Chem. Chem. Phys. **10**, 6615 (2008).
- ⁴¹ M. J. Frisch and G. W. Trucks and H. B. Schlegel and G. E. Scuseria and M. A. Robb and J. R. Cheeseman and G. Scalmani and V. Barone and B. Mennucci and G. A. Petersson and H. Nakatsuji and M. Caricato and X. Li and H. P. Hratchian and A. F. Izmaylov and J. Bloino and G. Zheng and J. L. Sonnenberg and M. Hada and M. Ehara and K. Toyota and R. Fukuda

and J. Hasegawa and M. Ishida and T. Nakajima and Y. Honda and O. Kitao and H. Nakai and T. Vreven and Montgomery, Jr., J. A. and J. E. Peralta and F. Ogliaro and M. Bearpark and J. J. Heyd and E. Brothers and K. N. Kudin and V. N. Staroverov and R. Kobayashi and J. Normand and K. Raghavachari and A. Rendell and J. C. Burant and S. S. Iyengar and J. Tomasi and M. Cossi and N. Rega and J. M. Millam and M. Klene and J. E. Knox and J. B. Cross and V. Bakken and C. Adamo and J. Jaramillo and R. Gomperts and R. E. Stratmann and O. Yazyev and A. J. Austin and R. Cammi and C. Pomelli and J. W. Ochterski and R. L. Martin and K. Morokuma and V. G. Zakrzewski and G. A. Voth and P. Salvador and J. J. Dannenberg and S. Dapprich and A. D. Daniels and O. Farkas and J. B. Foresman and J. V. Ortiz and J. Cioslowski and D. J. Fox. Gaussian 09 Revision A.02. Gaussian Inc. Wallingford CT 2009.

- ⁴² M. Kaupp and P. v. R. Schleyer and H. Stoll and H. Preuss, *J. Chem. Phys.* **94**, 1360 (1991).
- ⁴³ R. Krishnan and J. S. Binkley and R. Seeger and J. A. Pople, *J. Chem. Phys.* **72**, 650 (1980).
- ⁴⁴ M. J. Frisch and J. A. Pople and J. S. Binkley, *J. Chem. Phys.* **80**, 3265 (1984).
- ⁴⁵ T. Clark and J. Chandrasekhar and P. V.R. Schleyer, *J. Comput. Chem.* **4**, 294 (1983).
- ⁴⁶ P. M.W. Gill and B. G. Johnson and J. A. Pople and M. J. Frisch, *Chem. Phys. Lett.* **197**, 499 (1992).
- ⁴⁷ D. B. Kokh and R. J. Buenker and J. L. Whitten, *Surf. Sci.* **600**, 5104 (2006).
- ⁴⁸ A. Eichler and G. Kresse and J. Hafner, *Surf. Sci.* **397**, 116 (1998).
- ⁴⁹ G. Cilpa and M. Guitou and G. Chambaud, *Surf. Sci.* **602**, 2894 (2008).
- ⁵⁰ S. Andersson and L. Wilzén and M. Persson, *Phys. Rev. B* **38**, 2967 (1988).
- ⁵¹ S. Andersson and M. Persson and J. Harris, *Surf. Sci. Lett.* **360**, L499 (1996).
- ⁵² R. Bartlett and I. Grabowski and S. Hirata and S. Ivanov, *J. Chem. Phys.* **122**, 34104 (2005).
- ⁵³ G. J. Kroes and E. J. Baerends and R. C. Mowrey, *Phys. Rev. Lett.* **78**, 3583 (1997).
- ⁵⁴ G. H. Guvelioglu and P. Ma and X. He, *Phys. Rev. Lett.* **94**, 026103 (2005).

TABLE I: First layer interaction energy for the three processes. DFT calculations have been performed using SDD basis sets for the copper atoms and the large and diffuse 6-311++G(3df,3dp) basis for the hydrogen atoms. Data previously-obtained with periodic boundary conditions (PBC) are also reported.

	Physisorption			Barrier		Chemisorption		
	E/meV	Z/bohr	$d(\text{H-H})/\text{bohr}$	E/eV	Z/bohr	E/eV	Z/bohr	$d(\text{H-H})/\text{bohr}$
PW91	22.4	7.50	1.42	0.88	2.70	0.64	1.93	4.84
PBE0	6.5	8.30	1.41	1.02	2.65	0.53	1.96	4.72
B3LYP	1.1	9.70	1.40	1.26	2.65	0.54	1.94	4.77
B97-D	35.5	6.31	1.41	1.12	2.66	0.60	1.90	4.82
ω B97X	27.2	6.67	1.41	1.19	2.63	0.55	2.02	4.57
ω B97XD	30.5	6.43	1.41	1.16	2.63	0.57	1.98	4.63
M06-L	38.0	6.18	1.41	0.81	2.74	0.60	2.02	4.85
M06-2X	25.6	7.00	1.40	1.56	2.62	0.22	2.15	4.64
Other works								
MRCI+Q ^a	28.2	6.99	1.40	1.54	2.46	0.60	1.9	4.82
BP88-PBC	-	-	-	0.70 ^b	2.62 ^b	~0.5 ^b	2.0 ^b	4.82 ^b
	-	-	-	0.63 ^c	2.60 ^c	-	-	-
PW91-PBC	-	-	-	1.21 ^d	2.65 ^d			
	-	-	-	-	-	0.47 ^e	-	-
Expt. ^f	29.9-31.4	-	-	-	-	-	-	-

^a see Ref. 15; ^b see Ref. 7; ^c see Ref. 4; ^d see Ref. 8; ^e see Ref. 54; ^f see Ref. 50 and 51.

TABLE II: Second layer physisorption minimum ($\text{H}_2/\text{H}_2\text{Cu}_{13}$ system), considering both parallel and perpendicular approaches of the second H_2 molecule on the H_2Cu_{13} system. In parenthesis, results obtained with the SDD basis set.

	Parallel			Perpendicular		
	E/meV	Z/bohr	$d(\text{H-H})/\text{bohr}$	E/meV	Z/bohr	$d(\text{H-H})/\text{bohr}$
PW91	19.1	8.56	1.42	41.5	7.80	1.42
PBE0	5.2	9.24	1.41	22.2	8.03	1.41
B3LYP	0.3	10.11	1.40	13.4	8.65	1.40
B97-D	19.8	7.99	1.41	15.6	8.02	1.41
ω B97X	15.8	8.00	1.41	68.5	6.96	1.41
ω B97XD	16.1	8.25	1.40	45.9	7.11	1.41
M06-L	10.7	8.00	1.41	45.4	6.66	1.41
M06-2X	11.2	8.45	1.39	37.5	6.67	1.40
Other works						
MRCI ^a	57.0	6.42	1.40	111.7	6.41	1.40
MRCI+Q ^a	77.5	6.42	1.40	131.9	6.24	1.40

^a From ref 15.

Figure captions

FIG. 1: Definition of the *btb* dissociation pathway, H atoms (white circles) on the (100) surface of Cu (grey circles) are localized on the bridge sites. *btb* corresponds to an approach where G center of mass of H_2 is on a top site and the H atoms are dissociating on bridge sites.

FIG. 2: Sketches of the second layer interaction for (a) parallel and (b) perpendicular approaches. The convention for the atoms is the same as in Figure 1.

FIG. 3: Physisorption curves for the first H_2 layer interaction on the model Cu_{13} cluster (MRCI+Q data from Ref. 15).

FIG. 4: Second H_2 layer interaction curves, with both (a) parallel and (b) perpendicular approaches with respect to the first adsorbed layer (MRCI+Q data from Ref. 15).

Fig. 1: Cilpa *et al.*

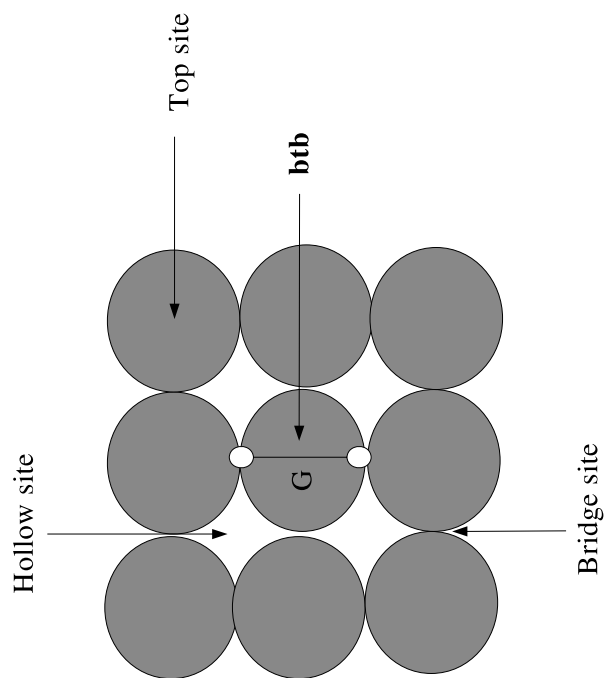


Fig. 2: Cilpa *et al.*

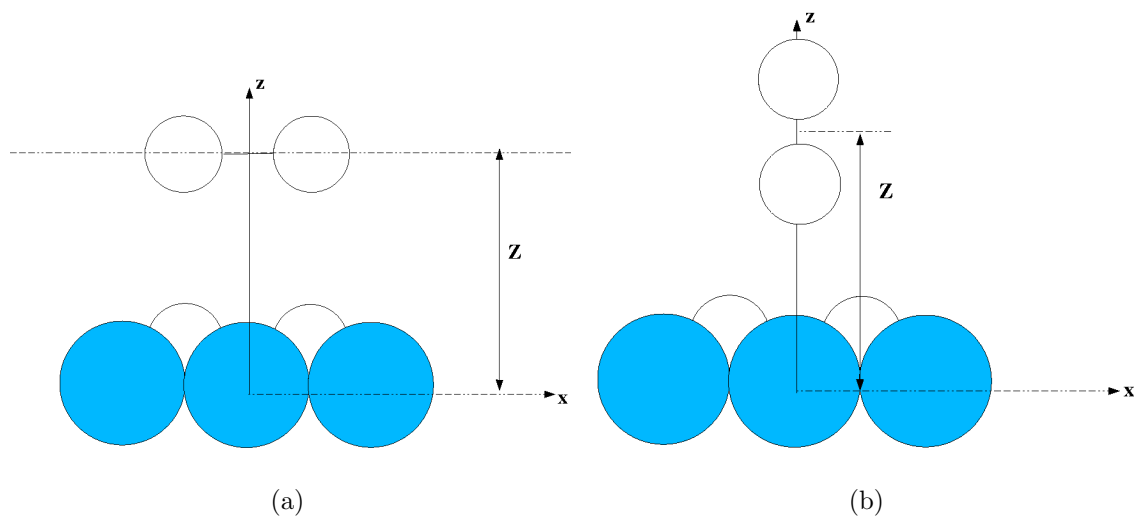


Fig. 3: Cilpa *et al.*

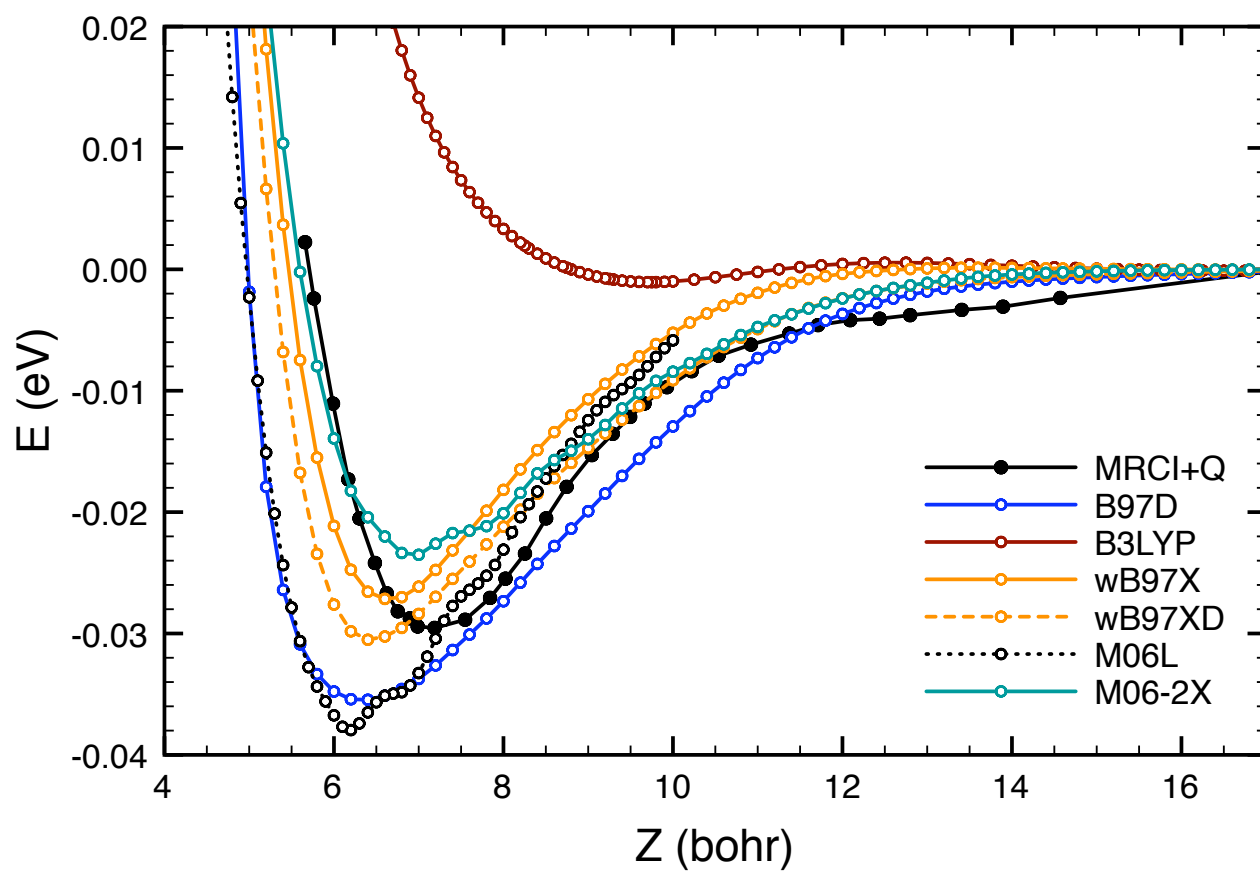
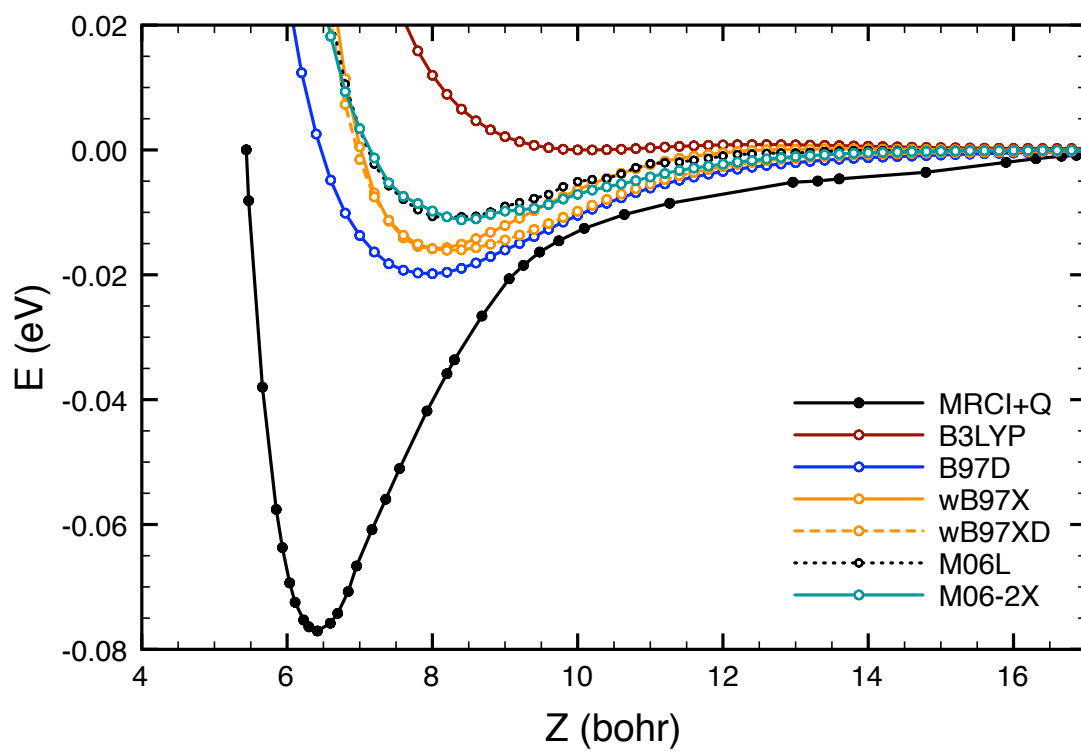
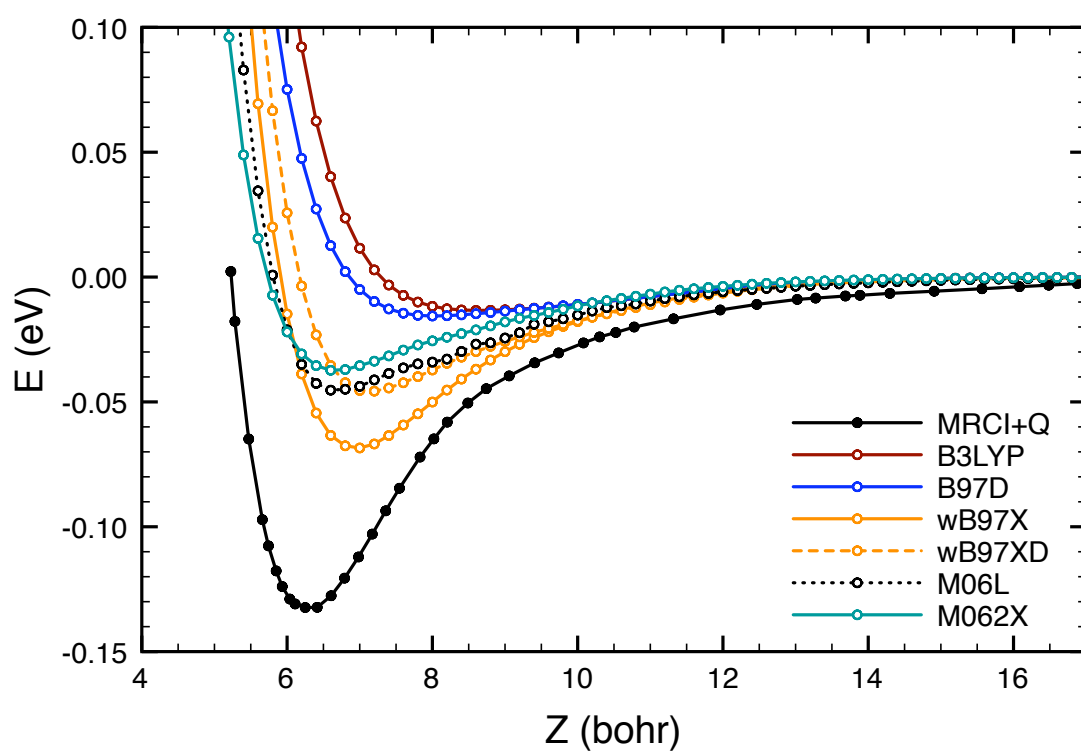


Fig. 4: Cilpa *et al.*



(a)



(b)